Accurate 3-D Imaging Method Based on Range Points Migration for 140GHz-band Radar

Yuta Sasaki, Shouhei Kidera and Tetsuo Kirimoto
Graduate School of Informatics and Engineering, The University of Electro-Communications, Tokyo, Japan
e-mail : sasaki@secure.ee.uec.ac.jp

***Abstract*—Ultra-wideband (UWB) millimeter wave radar has a great advantage for achieving higher spatial resolution and is promising for collision avoidance or target recognition in short range sensing issue. In this paper, we focus on the 140-GHz band radar system, which has a significant advantage for wider frequency range and more compact radar module. For such application, we have originally developed an accurate and high-speed imaging method named as range points migration (RPM), which is based on a 3-D target boundary extraction scheme. This paper introduces the existing RPM radar to achieve fast data acquisition with multiple receivers. To enhance a computational cost and accuracy, we newly introduce the pre- and post-processing algorithms for the original multi-static RPM method, as range points selection and isolated points elimination. Results from numerical simulations assuming 140 GHz radar system, demonstrate that the proposed method accomplishes more efficient 3-D imaging compared with that obtained by the original RPM method.**

***Index Terms*—UWB radar, Range points migration, Multi-static UWB Radar, Millimeter wave radar, Short range sensing.**

I. INTRODUCTION

The short range sensing with a millimeter wave radar system has a great potential to be a next innovative sensor, because it is applicable to the situation in the optical sensor cannot be applicable, such as adverse weather, smog or darkness, where the optical sensor cannot be used. Particularly, this radar system is promising for the applications such as collision avoidance sensor for vehicle, or watch sensors for independently living elderly or disabled persons. Nowadays, the 140 GHz band radar system comes under the spotlight because of providing wider frequency band around 10 GHz. Moreover, the transmitting and receiving modules become considerably downsized using such higher frequency, which contributes a flexibility at the actual implementing. In addition, such RF module will be available in near future, where the CMOS based architecture is now developed in related corporations.

There are intensive studies for radar imaging method assuming short range sensing situation, based on data synthesis, such as synthetic aperture radars (SAR) [1], time-reversal algorithms [2], or range migration methods [3]. However, this type of methods has plural drawbacks, that its computational burden becomes impractically large, particularly for 3D problems due to delay-and-sum approach for each pixel, or that the spatial resolution is strictly limited by the signal bandwidth and wavelength. In contrast, as a fast non-parametric 3-D imaging method, the SEABED (shape estimation algorithm based on boundary scattering transform and extraction of directly scattered waves) method has been developed, which is based on reversible transforms between the time delay and the target boundary [4]. However, this method has serious drawbacks that it is considerably sensitive for observed range errors due to the use of derivative operation. It also requires a connection process of range points, which is often a difficult task in the complicated-shaped or multiple object case due to richly interfered signals. As an essential solution for this difficulty, the RPM (range points migration) method has been proposed [5]. This method is based on scattering center point (target point) extraction from corresponding range point (a set of antenna location and measured range) by calculating DOA (direction of arrival), which is derived from the distribution function generated by other range points. As a notable feature of this method, it accomplishes direct and fast mapping from observed range points to target boundary points without any connecting process, and retains both high accuracy and lower computational cost, even in complicated-shaped or multiple target boundaries by avoiding the task of waveform summation or derivative operations. Moreover, there are several extension studies of this method, for complex-shape target imaging [8] or acoustic biomedical imaging applications [7].

This paper focuses on 140GHz-band radar system, which has a great potential for achieving higher range resolution and compact radar module. In particular, the multi-static radar with array antennas, is assumed in this paper, which is applicable to moving target imaging with less data acquisition time compared with a radar scanning model. The multi-static extension of the RPM has been already proposed in [5], and been verified for accomplishing accurate moving target imaging with the motion estimation. However, this method has a severe problem for computational cost in the case of multiple targets. This is because the multi-static RPM requires a numerous computational cost for calculating intersection points of multiple ellipsoids (foci are transmitting and receiving antenna locations, and major diameter is range) to determine a target boundary point. To accelerate the imaging process, this paper introduces the pre-processing algorithm for selecting necessary range points by the criteria derived from the geometrical condition established between sensor and target locations. Furthermore, in the case of richly interfered situation, the reconstruction accuracy considerably degrades due to the DOA estimation error in the RPM method. To enhance the accuracy, this paper also introduces the post-processing algorithm based on an elimination of isolated points.

Results obtained from the geometrical optics (GO) based numerical simulation, that the proposed method remarkably enhances both computational cost and accuracy, compared with the SAR and the original RPM.

II. SYSTEM MODEL

Figure 1 shows the system model. It assumes that each target has an arbitrary 3-D shape with a clear boundary. A number of omni-directional antennas are arranged in an array on the

978-1-4673-6555-0/15/$31.00 ©2015 IEEE

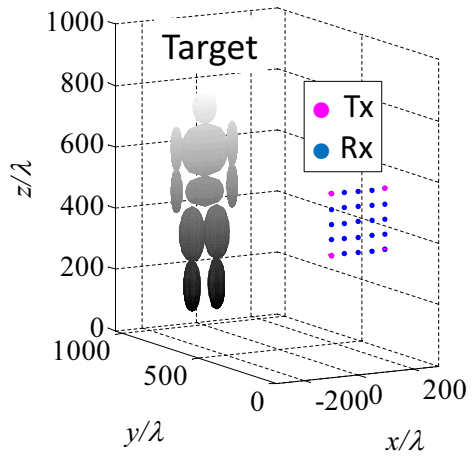

Fig. 1. System model.

$y = 0$ plane to form a multi-static radar configuration. The locations of the transmitting and receiving antennas are defined as $\boldsymbol{L}_T = (X_T, 0, Z_T)$ and $\boldsymbol{L}_R = (X_R, 0, Z_R)$, respectively. For each combination of $\boldsymbol{L}_{\mathrm{T}}$ and $\boldsymbol{L}_{\mathrm{R}}$, the output of the Wiener filter is denoted as $s(\boldsymbol{L}_{\mathrm{T}}, \boldsymbol{L}_{\mathrm{R}}, R')$, where $R' = \mathrm{c}\tau/2$ is defined using the delay time τ and the radio wave speed c. $\boldsymbol{q} = (\boldsymbol{L}_{\mathrm{T}}, \boldsymbol{L}_{\mathrm{R}}, R)^T$ is defined as the range point, which is extracted from the local maxima of $s(\boldsymbol{L}_{\mathrm{T}}, \boldsymbol{L}_{\mathrm{R}}, R')$ to R'. This procedure is detailed in [5].

III. Conventional 3-D Imaging Method

Focusing on 3-D short range imaging issue, various type of target shape reconstruction methods have been proposed. Synthetic aperture radar (SAR) is one of the most powerful tools even in short range sensing issue. Although the SAR or other waveform focusing approaches, such as time reversal or range migration methods, provide accurate image for point-wise target, there are severe limitations that it cannot offer a sufficient accuracy for non-pointwise target, and its computational cost becomes enormous in 3-D imaging due to signal synthesizing approach with all received signals in each voxel evaluation. As a different approach, the SEABED method has been proposed, which specifies the target boundary extraction using extracted range points. This method employs a reversible transform established between target boundary and range curve (quasi-wavefront), and accomplishes fast 3-D imaging for arbitrary target shape. However, this method has a serious problem that it requires the complicated pre-processing for generating quasi-wavefront by connecting range points.In addition, due to employing the derivative operation in the transform, it also suffers from serious errors enhanced by the small range fluctuation.

IV. Proposed Method

A. Original Multi-static RPM Method

As an efficient solution for the aforementioned problem, the RPM method has been established [5]. In addition, this method has been extended to multi-static observation model [6]. This method assumes that a target boundary point exists on an ellipsoid, whose focal points are $\boldsymbol{L}_T$ and $\boldsymbol{L}_R$ and major radius is R. For extracting the target point, this method employs the basis that the actual target boundary point should be included in all the possible intersection points determined by other range points. For determining a target point corresponding to a range point $\boldsymbol{q}_i$, this method extracts an optimal intersection points as $\boldsymbol{p}(\boldsymbol{q}_i)$ by assessing the spatial accumulation of intersection points as;

$$\hat{\boldsymbol{p}}(\boldsymbol{q}_i) = \underset{\boldsymbol{p}^{\mathrm{int}}(\boldsymbol{q}_i;\boldsymbol{q}_l,\boldsymbol{q}_m)\in\mathcal{P}_i}{\arg\max} \sum_{(\boldsymbol{q}_j,\boldsymbol{q}_k)\in\mathcal{Q}_i} g(\boldsymbol{q}_i;\boldsymbol{q}_j,\boldsymbol{q}_k) \times \exp\left\{-\frac{||\boldsymbol{p}^{\mathrm{int}}(\boldsymbol{q}_i;\boldsymbol{q}_j,\boldsymbol{q}_k) - \boldsymbol{p}^{\mathrm{int}}(\boldsymbol{q}_i;\boldsymbol{q}_l,\boldsymbol{q}_m)||}{2\sigma_r^2}\right\}. \quad (1)$$

where $p^{\mathrm{int}}(\boldsymbol{q}_i;\boldsymbol{q}_j,\boldsymbol{q}_k)$ denotes the intersection points among the three ellipsoids, determined by the range points $\boldsymbol{q}_i, \boldsymbol{q}_j$, and $\boldsymbol{q}_k$, σ_r is determined by considering the spatial density of the accumulated intersection points. $\mathcal{P}_i$ denotes a set of all intersection points for $\boldsymbol{q}_i$, evaluated by $\mathcal{Q}_i$, which denotes a set of possible combination of range points. The weighting function $g(\boldsymbol{q}_i;\boldsymbol{q}_j,\boldsymbol{q}_k)$ is defined by

$$g\left(\boldsymbol{q}_i;\boldsymbol{q}_j,\boldsymbol{q}_k\right) = s\left(\boldsymbol{q}_j\right)\exp\left\{-\frac{D\left(\boldsymbol{q}_i,\boldsymbol{q}_j\right)}{2\sigma_D^2}\right\} + s\left(\boldsymbol{q}_k\right)\exp\left\{-\frac{D\left(\boldsymbol{q}_i,\boldsymbol{q}_k\right)}{2\sigma_D^2}\right\}. \quad (2)$$

where, σ_D is determined empirically and $D(\boldsymbol{q}_i,\boldsymbol{q}_j)$ denotes the actual separation of two set of transmitting and receiving antennas as;

$$D(\boldsymbol{q}_i,\boldsymbol{q}_j) = \min\left(\|\boldsymbol{L}_{\mathrm{T},i} - \boldsymbol{L}_{\mathrm{T},j}\|^2 + \|\boldsymbol{L}_{\mathrm{R},i} - \boldsymbol{L}_{\mathrm{R},j}\|^2,\ \|\boldsymbol{L}_{\mathrm{T},i} - \boldsymbol{L}_{\mathrm{R},j}\|^2 + \|\boldsymbol{L}_{\mathrm{R},i} - \boldsymbol{L}_{\mathrm{T},j}\|^2\right). \quad (3)$$

The weighting function in Eq. (2) considers that the scattering center moves along the target boundary (not point target) corresponding to antenna location.

In general, the computation cost for calculating intersection point of three ellipsoids is considerably higher than that of three spheres (corresponding to mono-static radar). In addition, while the original RPM method eliminates the false target points by reassessing the evaluation function denoted in the right term of Eq. (1) with a constant threshold [5]. In richly interfered situation, caused by closely spaced multiple targets case, this process cannot eliminate the false point completely, and it suffers from the inaccuracy for target recognition.

B. Acceleration by Range Points Selection

As an acceleration approach of the original RPM, this paper newly introduces the pre-processing algorithm for range points (abbreviated as RP) selection. As described before, for target point extraction at main range point (called MainRP, $\boldsymbol{q}_i$ in Eq. (1)), the RPM needs to evaluate the accumulation degree of intersection points of ellipsoids defined by other range points (called SubRPs, $\boldsymbol{q}_j, \boldsymbol{q}_k$ in Eq. (1)). However, in this evaluation, the number of SubRPs seriously affects an computational cost due to numerical solution for intersection point of ellipsoid. In multiple target cases, if the MainRP corresponds to the target point in the n-th target (denoted as MainRP_n), the SubRPs also should correspond to those of the n-th target (denoted as SubRP_n). For an accurate reconstruction of target point, we only evaluate a set of SubRP_n, and other RPs has possibility to introduce the error in final image. However, it is essentially

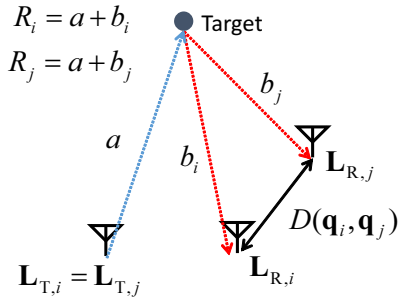

Fig. 2. Geometrical condition for range points selection.

difficult to recognize the target number for each range point, beforehand. Instead of this, this paper eliminates the the range points from SubRPs as;

$$|R_i - R_j| > D(\boldsymbol{q}_i, \boldsymbol{q}_j). \tag{4}$$

Here, it assumes that $\boldsymbol{L}_T$ in all comparing RP are same. This elimination is based on the assumption that if the SubRPs corresponds to the same target number of the MainRP, the range difference should be smaller than $D(\boldsymbol{q}_i, \boldsymbol{q}_j)$. This condition is easily derived from the geometrical condition for general triangle as shown in Fig. 2. Then, the set of SubRPs $\mathcal{Q}_i$, denoted in Eq. (1), is redefined as;

$$\begin{aligned}\mathcal{Q}_i = \{\ (\boldsymbol{q}_j, \boldsymbol{q}_k)\ |\ \ & \boldsymbol{L}_{T,i} = \boldsymbol{L}_{T,j} = \boldsymbol{L}_{T,k}, \\ & |R_i - R_j| < D(\boldsymbol{q}_i, \boldsymbol{q}_j), |R_i - R_k| < D(\boldsymbol{q}_i, \boldsymbol{q}_j)\ \ \}.\end{aligned} \tag{5}$$

Figure 3 shows the set of SubRPs$\mathcal{Q}_i$ for MainRP$_i$, which is selected by the proposed method.

C. Elimination for Isolated Points

To enhance the total accuracy of the RPM target points, this paper also introduces false target point elimination scheme after the RPM imaging process. This approach is based on the property that the surrounding area of actual target point includes a certain number of target points, because an actual distribution of target points should focus on the local area of a target boundary, if a target has a convex shape locally. Based on this well-established assumption, the proposed method eliminates the target points $\hat{\boldsymbol{p}}(\boldsymbol{q}_i)$ if it satisfies the following equation.

$$\begin{aligned} & n(\mathcal{P}_i^{\mathrm{sel}}) < n_0 \\ & \mathcal{P}_i^{\mathrm{sel}} \equiv \{\ \hat{\boldsymbol{p}}(\boldsymbol{q}_j)\ |\ \ \|\hat{\boldsymbol{p}}(\boldsymbol{q}_i) - \hat{\boldsymbol{p}}(\boldsymbol{q}_j)\| < \epsilon_{\mathrm{elm}}\} \end{aligned} \tag{6}$$

where $n(A)$ expresses the number of elements included in set A, ϵ_{elm} and n_0 are empirically determined thresholds. If this condition is satisfied, the target point is regarded as the isolated point, and is eliminated.

D. Procedure of the Proposed Method

Figure 4 shows the flowchart of the proposed RPM. The procedure is as follows:

1) Observed data are acquired as the Wiener filter outputs $s(\boldsymbol{L}_T, \boldsymbol{L}_R, R')$.
2) Range points $\boldsymbol{q}_i$ are extracted from the Wiener filter outputs.
3) For each MainRP, the set of necessary SubRPs $\mathcal{Q}_i$ is extracted through Eq. (5).

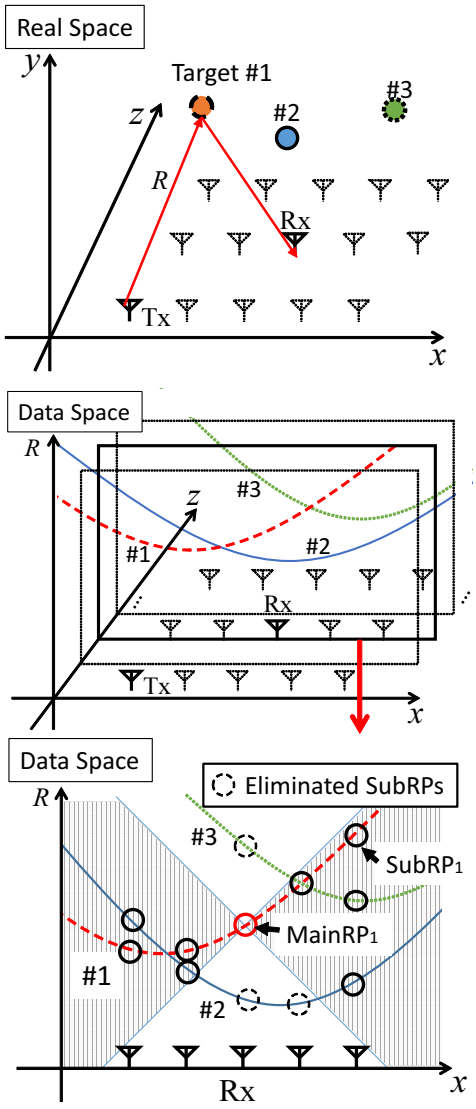

Fig. 3. Relationship between target point and corresponding range points.

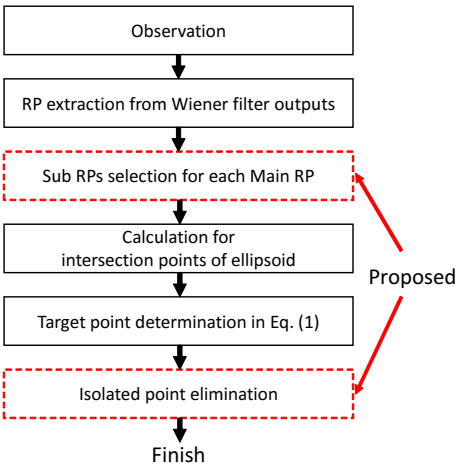

Fig. 4. Flowchart of the proposed method.

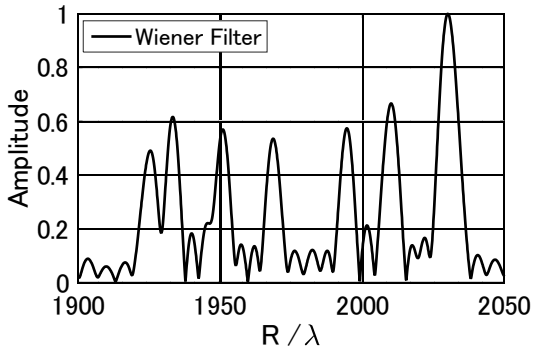

Fig. 5. Example of Wiener filter output.

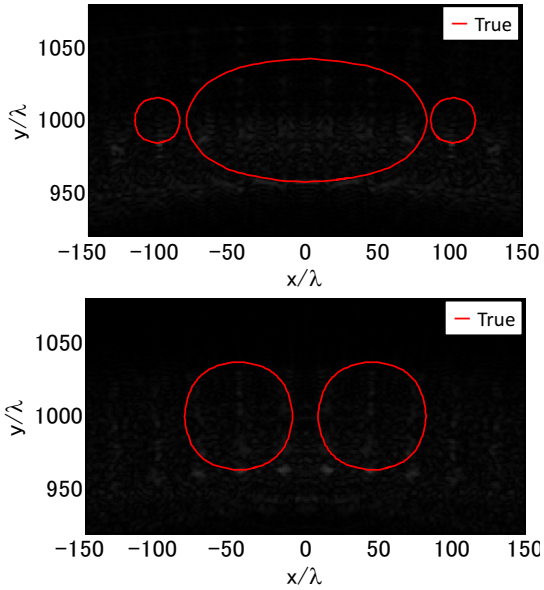

Fig. 6. Cross-section image of SAR, $z = 560\lambda$ (upper) and $z = 330\lambda$ (lower).

4) Target point $\hat{\boldsymbol{p}}(\boldsymbol{q}_i)$ is determined for each $\boldsymbol{q}_i$ evaluating for accumulation of intersection points with $\mathcal{Q}_i$ in Eq. (1).
5) Target points are determined for all $\boldsymbol{q}_i$ by repeating Step 3 and 4 .
6) False target points elimination by threshold processing in Eq. (6) .

V. PERFORMANCE EVALUATION IN NUMERICAL SIMULATIONS

This section describes the performance evaluation of the proposed method through numerical simulations, comparing other imaging methods. In this simulation, the transmitted signal is set as the pulse modulated signal, whose center frequency is 140 GHz, and effective bandwidth is 10 GHz. The theoretical range resolution in the air is 15 mm. The center wavelength is 2.1 mm. It assumes that a target is human body approximated by an aggregate of 11 ellipsoids, expressing head, upper and lower body, arms and legs as in Fig. 1. The numbers of transmitting and receiving antennas are 4 and 25, respectively. The array arrangement is also shown in Fig. 1, where the minimum array spacing is 50 λ. The received data are generated by geometrical optics (GO) approximation. A noiseless situation is assumed. First, Figure. 5 shows the

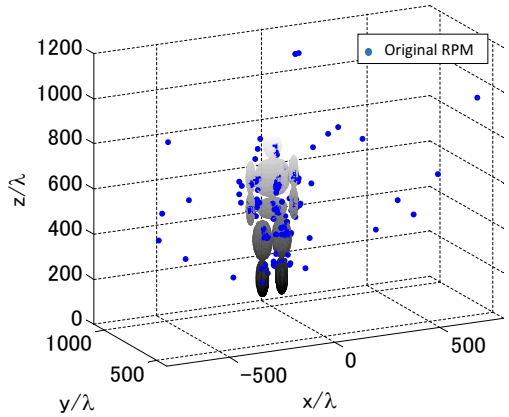

Fig. 7. Target points obtained by the original multi-static RPM method.

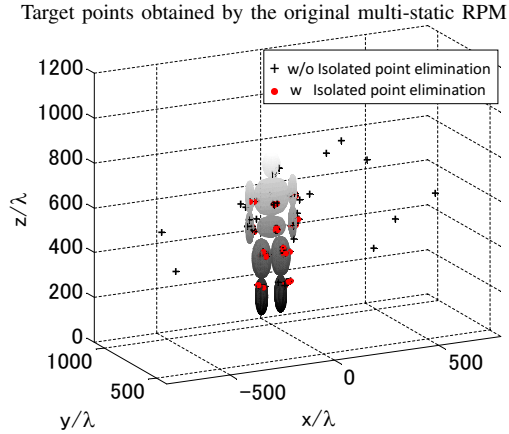

Fig. 8. Target points obtained by the proposed RPM method with or without isolated point elimination.

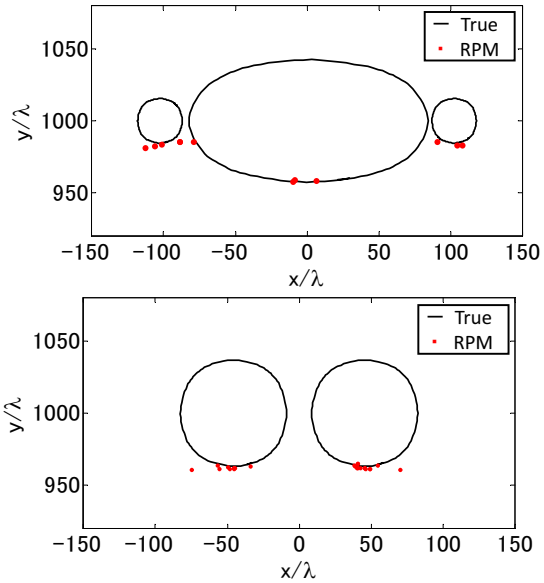

Fig. 9. Cross-section image of the proposed RPM, $z = 560\lambda$ (upper) and $z = 330\lambda$ (lower).

example of output of Wiener filter for the received signal, where the transmitting and receiving antennas are located as $(-100, 0, 400)$ and $(-100, 0, 400)$, respectively.

As the method comparison, the imaging results obtained by SAR is investigated. Here, the complex signal is generated by the Hilbert transform of each received signal, and its image is generated by the back projection algorithm. Figure 6 shows a cross section images reproduced by SAR at abdominal and femoral areas, where each imaging voxel size is 1.0λ. This figure indicates that, in any area, there are unnecessary responses around the actual target boundaries due to grating lobe caused by sparse sampling of array antennas. Consequently, it is difficult to capture the shape of human body. Moreover, it costs more than 300 hours to reconstruct a full 3-D image with Intel Xeon CPU E5-1620 (3.6 GHz) processor with 1.0 lambda voxel spacing for the range $-150 \leq x \leq 150$, $900 \leq y \leq 1100$, $0 \leq z \leq 800$. Figure 7 shows the target boundary points obtained by the original multi-static RPM method. This figure demonstrates that there are many target points far from the actual target boundary in spite of introducing the elimination based on the RPM evaluation function. It costs 6230 sec to generate the full 3-D image by this method, which is 150 times faster than that cost in SAR. On the contrary, Fig. 8 shows the target boundary points obtained the proposed method with or without eliminating process for the isolated point, described in Sec. IV-C. In this case, the calculation time is around 3200 sec, around two times faster than that in the original RPM method. This is because the redundant SubRPs are considerably eliminated through the RP selection process, described in Sec. IV-B. This figure also denotes that the elimination process for isolated point remarkably suppresses inaccuracy target points.

For the quantitative evaluation of reconstruction accuracy, the error value for $e(\boldsymbol{p}_i^{\mathrm{est}})$ is introduced as

$$e(\boldsymbol{p}_i^{\mathrm{est}}) = \min_{\boldsymbol{p}^{\mathrm{true}}} \|\boldsymbol{p}_i^{\mathrm{est}} - \boldsymbol{p}^{\mathrm{true}}\|_2, \qquad (i = 1, 2, \cdots, N_{\mathrm{T}}). \quad (7)$$

where $\boldsymbol{p}_i^{\mathrm{est}}$ and $\boldsymbol{p}^{\mathrm{true}}$ express the location of the true target and the estimated target point, respectively. N_{T} is the total number of $\boldsymbol{p}_i^{\mathrm{est}}$. Figure 10 plots the cumulative distribution of this error value for each method. The total numbers of estimated target points N_{T} are 159 for the original RPM and 112 for the proposed method, respectively. This result shows that 75% of the estimated target points obtained by RPM satisfies $e(\boldsymbol{p}_i^{\mathrm{est}}) < 10\lambda$. On the contrary, 88% of those obtained by the proposed method, satisfies $e(\boldsymbol{p}_i^{\mathrm{est}}) < 10\lambda$ (around 20mm in this model.). This evaluation quantitatively verifies the effectiveness of the proposed method in terms of reconstruction accuracy.

VI. CONCLUSION

This paper proposed an efficient 3-D imaging method for 140GHz-band millimeter wave radar by adding the pre and post processing for the original multi-static RPM method. In particular, this paper introduced the pre-processing algorithm as range points selection, where unnecessary range points are removed for each target point extraction. To enhance the reconstruction accuracy, the post-processing algorithm as isolated points elimination was adopted for reducing a false image caused by interference effect. The results of the numerical simulations with geometrical optics approximation,

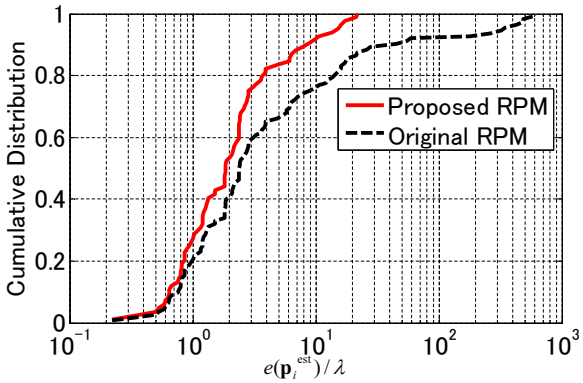

Fig. 10. Cumulative distribution for reconstruction error.

demonstrated that the range points selection algorithm considerably accelerated 3-D imaging process with maintaining the accuracy, and its calculation time is around 200 and 2 times faster than those in SAR and the original RPM. Moreover, the isolated points elimination remarkably reduces the inaccurate target points using a simple thresholding. The experimental verification is our future work.

ACKNOWLEDGMENT

This work was supported by the project "140 GHz band accurate radar system" promoted by Japanese Ministry of Internal Affairs and Communications, Japan.

REFERENCES

[1] D. L. Mensa, G. Heidbreder and G. Wade, "Aperture Synthesis by Object Rotation in Coherent Imaging," *IEEE Trans. Nuclear Science*, vol. 27, no. 2, pp. 989-998, Apr., 1980.

[2] A. J. Devaney, Time Reversal Imaging of Obscured Targets From Multistatic Data, *IEEE Trans. Antennas Propag.*, vol. 53, no. 5, pp. 1600–1610, May, 2005.

[3] J. Song, Q. H. Liu, P. Torrione, and L. Collins, Two-dimensional and three dimensional NUFFT migration method for landmine detection using ground-penetrating radar, *IEEE Trans. Geosci. Remote Sens.*, vol. 44, no. 6, pp. 1462–1469, Jun, 2006.

[4] T. Sakamoto, T. Sato, "A Target Shape Estimation Algorithm for Pulse Radar Systems Based on Boundary Scattering Transform," *IEICE Trans. Commun.*, vol. E87-B, no. 5, pp. 1357-1365, July, 2004.

[5] S. Kidera, T. Sakamoto and T. Sato, "Accurate UWB Radar 3-D Imaging Algorithm for Complex Boundary without Wavefront Connection," *IEEE Trans. Geosci. and Remote Sens.*, vol. 48, no. 4, pp. 1993-2004, Apr., 2010.

[6] R. Yamaguchi ,S. Kidera and T. Kirimoto, "Nonparametric UWB Radar Imaging Algorithm for Moving Target Using Multi-static RPM Approach," *Asia-Pacific Conference on Synthetic Aperture Radar (APSAR) 2011*, Seoul, Korea, pp. 275-278, Sep., 2011.

[7] H. Taki, S. Tanimura, T. Sakamoto, T. Shiina, T. Sato, "Accurate ultrasound imaging based on range point migration method for the depiction of fetal surface," *The Japan Society of Ultrasonics in Medicine 2014*, pp. 51-58, Sep., 2014.

[8] R.Salman, I. Willms "3D UWB Radar Super-Resolution Imaging for complex Objects with discontinous Wavefronts," *IEEE International Conference on Ultra-Wideband (ICUWB) 2011*, pp. 346-350, 2011